Am J Cardiovasc Dis 2023;13(5):309-319
www.AJCD.us /ISSN:2160-200X/AJCD0152641

Original Article

Association of coronary plaque morphology with inflammatory biomarkers and target lesion revascularization in patients with chronic coronary syndrome: an optical coherence tomography study

Kohei Saiin[1*], Takao Konishi[1*], Sho Kazui[1], Yutaro Yasui[1], Yuki Takahashi[1], Seiichiro Naito[1], Sakae Takenaka[1], Yoshifumi Mizuguchi[1], Atsushi Tada[1], Yuta Kobayashi[1], Yoshiya Kato[1], Kazunori Omote[1], Takuma Sato[1], Kiwamu Kamiya[1], Toshiyuki Nagai[1], Shinya Tanaka[2,3], Toshihisa Anzai[1]

[1]Department of Cardiovascular Medicine, Faculty of Medicine and Graduate School of Medicine, Hokkaido University, Sapporo, Hokkaido, Japan; [2]Department of Cancer Pathology, Faculty of Medicine, Hokkaido University, Sapporo, Hokkaido, Japan; [3]Institute for Chemical Reaction Design and Discovery (WPI-ICReDD), Hokkaido University, Sapporo, Hokkaido, Japan. [*]Equal contributors.

Received August 5, 2023; Accepted October 7, 2023; Epub October 15, 2023; Published October 30, 2023

Abstract: Background: The characteristics of high-risk coronary atherosclerosis evaluated using optical coherence tomography (OCT) can have a prognostic role. Inflammatory biomarkers may be related to the severity of coronary artery disease. This study investigated the association of high-risk morphological features of coronary plaques on OCT with circulating levels of inflammatory biomarkers and target lesion revascularization (TLR). Materials and Methods: We prospectively analyzed the data of 30 consecutive patients with chronic coronary syndrome who underwent percutaneous coronary intervention (PCI) using OCT. The levels of interleukin-6, tumor necrosis factor-alpha, high-sensitivity C-reactive protein, pentraxin 3, vascular endothelial growth factor, and monocyte chemoattractant protein-1 (MCP-1) were measured in plasma samples. Coronary plaque characteristics were scored quantitatively in the form of coronary plaque risk score (CPRS). The estimated high-risk plaque characteristics for TLR were plaque rupture, plaque erosion, calcified nodule, lipid-rich plaque, thin-cap fibroatheroma, cholesterol crystals, macrophage infiltration, microchannels, calcification angle >90°, and microcalcifications. Each high-risk feature carries 1 point. Patients were defined as having a low CPRS (CPRS ≤3) or a high CPRS (CPRS ≥4). Results: The primary outcome was TLR. TLR occurred in 6 (20%) patients within 15 months of PCI. High CPRS on OCT was directly correlated with TLR (P=0.029). In logistic regression analysis, CPRS was associated with TLR (odds ratio, 10.0; 95% confidence interval, 1.34-74.5). Serum MCP-1 level was significantly correlated with the CPRS (P=0.020). Conclusions: In patients with chronic coronary syndrome, CPRS may be a surrogate predictor of TLR. Serum MCP-1 may aid in the detection of high-risk coronary atherosclerosis.

Keywords: Chronic coronary syndrome, optical coherence tomography, target lesion revascularization, percutaneous coronary intervention, biomarker

Introduction

In many developed countries, coronary artery disease (CAD) is one of the most common causes of death, and chronic coronary syndrome (CCS) is the most common initial symptom. Despite the contemporary evolution of percutaneous coronary intervention (PCI) using drug-eluting stenting and a drug-coated balloon, restenosis and repeat revascularization remain major concerns and limit the efficacy of PCI in patients with CCS [1, 2].

Optical coherence tomography (OCT) is a useful intravascular imaging modality that uses the reflection of near-infrared light to create images. Recently, several OCT studies have identified the characteristics of high-risk coronary plaques and evaluated the risks of adverse cardiovascular events [3-5]. Lipid-rich plaques

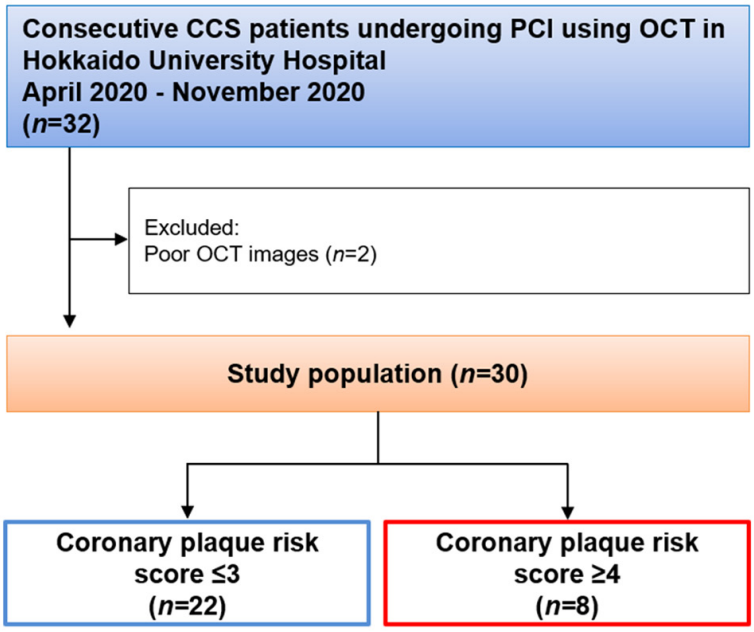

Figure 1. Flow diagram of the study. CCS, chronic coronary syndrome; PCI, percutaneous coronary intervention; OCT, optical coherence tomography.

identified using OCT in the non-culprit segment of the target vessel have been demonstrated to be associated with a higher incidence of a composite of cardiac death, acute myocardial infarction, and repeated revascularization [5]. Thin-cap fibroatheroma (TCFA) could be an indicator of adverse cardiac events in patients with diabetes mellitus (DM) [4]. Macrophage infiltration is more abundant in the coronary arteries in patients with DM and acute coronary syndrome than in those without DM [6]. Consequently, several plaque characteristics identify high-risk plaques that are prone to future events. Therefore, it is clinically useful to evaluate and comprehensively quantify the morphological characteristics of high-risk coronary plaques - which may be associated with future cardiovascular events - using the coronary plaque risk score (CPRS) based on OCT.

Previous studies have demonstrated that inflammatory cells, cytokines, and reactions play an important role in the progression of atheromas, plaque instability, and restenosis after revascularization [7-9]. Inflammatory biomarkers, such as interleukin (IL)-1, IL-6, tumor necrosis factor-alpha (TNF-α), monocyte chemoattractant protein-1 (MCP-1), high-sensitivity C-reactive protein (hs-CRP), vascular endothelial growth factor (VEGF), and pentraxin 3 have been reported to predict future cardiovascular events [8, 9]. Although the relationship between inflammatory biomarkers and clinical cardiovascular events has been elucidated, gaps in the knowledge of their correlation remain.

The aim of this study was to investigate whether CPRS based on OCT is associated with TLR and identify the inflammatory biomarkers that can help detect high-risk coronary plaques in patients with CCS.

Methods

Study design

Data from patients with CCS who underwent PCI using OCT at the Hokkaido University Hospital between April 2020 and November 2020 were prospectively analyzed. The study protocol was approved by the ethics committee of the Hokkaido University Hospital (approval no.: 019-0152). The patients provided informed consent to participate in this study.

Study population

Of 32 consecutive patients with CCS who underwent PCI using OCT, two patients with poor OCT image quality were excluded due to artifact. Consequently, 30 patients were examined in this study (**Figure 1**).

OCT and analysis

An OCT catheter (Dragon Fly; Abbott, Santa Clara, CA, USA) was proceeded using a 0.014-inch guidewire with the support of a 6- or 7-Fr guiding catheter. The imaging core was placed at the distal site of the lesion. OCT images were obtained using a continuous flush of contrast agent or low-molecular-weight dextran, and the OCT wire was pulled back at a rate of 18 mm/s. Although the OCT images were obtained without dilatation using a balloon, the lesion was dilated using a small balloon when the OCT catheter could not advance to the lesion

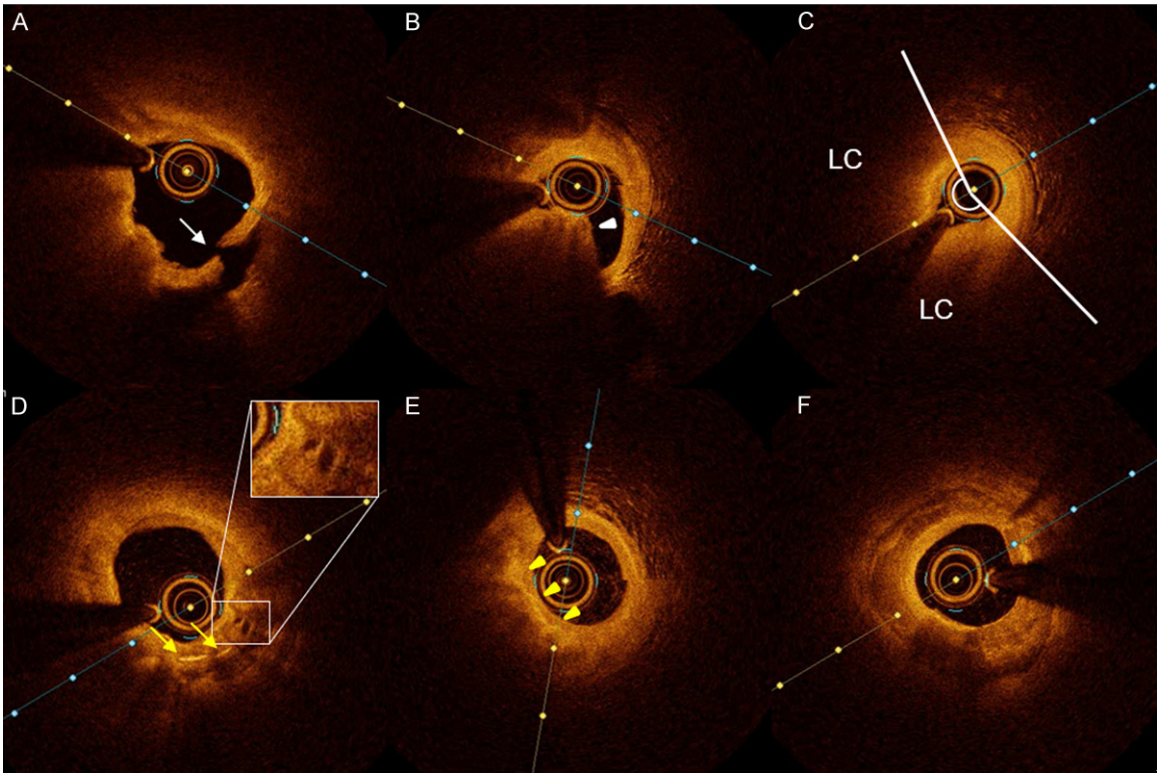

Figure 2. Representative optical coherence tomography (OCT) images of coronary artery plaques. A. Plaque rupture (white arrow); B. Calcified nodule (white arrowhead); C. Lipid-rich plaque; LC, lipid core; D. Cholesterol crystals (yellow arrows) and microchannels; E. Macrophage infiltration (yellow arrowheads); F. Calcification.

because of severe calcification or stenosis. The morphology of target lesions was analyzed. After identifying the most stenotic lesion, images of 5 mm of proximal and distal lesions (total length, 10 mm) were retained for further examination. Cross-sectional OCT images were analyzed at every 1 mm for plaque characteristics.

OCT definitions

According to the consensus standards for acquisition and measurement of intravascular optical coherence tomography studies, the coronary plaque characteristics were defined as follows [10]. Plaque rupture was defined as the presence of a fibrous cap discontinuity resulting in a cavity in the plaque (**Figure 2A**) [10]. Plaque erosion was defined as an intraluminal thrombus on an intact intima without plaque rupture [11]. Calcified nodules were defined as the disruption of a fibrous cap identified over a calcific plaque characterized by the protrusion of calcification or superficial calcium near substantive calcium proximal and/or distal to the lesion (**Figure 2B**) [11]. Lipid-rich plaques were defined as plaques with a maximal lipid arc >180° (**Figure 2C**) [10]. TCFA was defined as the presence of a thin fibrous cap (<65 μm) overlying a lipid-rich plaque [10]. Cholesterol crystals (CCs) were defined as thin and linear structures of high signal intensity within the lipid-rich plaque without attenuation (**Figure 2D**) [10]. Macrophage infiltration was defined as a region with high luminance near or within the fibrous cap accompanied by heterogeneous backward shadowing (**Figure 2E**) [10]. Microchannels were defined as small black holes with diameters of 50-300 μm within a plaque (**Figure 2D**) [10]. Calcification was defined as a well-delineated heterogeneous region with a low backscattering signal (**Figure 2F**) [10]. Microcalcifications were defined as calcium regions with angle <22.5° and length <1 mm [12]. Coronary plaque characteristics were scored quantitatively in the form of CPRS. The following were the high-risk plaque characteristics for TLR: plaque rupture, plaque erosion, calcified nodule, lipid-rich plaque, TCFA,

Table 1. Coronary plaque morphologies detected by OCT

Variable	Overall (n=30)
Plaque rupture, n (%)	3 (10)
Plaque erosion, n (%)	0
Calcified nodule, n (%)	3 (10)
Lipid-rich plaque, n (%)	17 (57)
Thin-cap fibroatheroma, n (%)	1 (3)
Macrophage infiltration, n (%)	26 (87)
Cholesterol crystals, n (%)	5 (17)
Microchannels, n (%)	20 (67)
Calcification >90°, n (%)	8 (27)
Microcalcification, n (%)	9 (30)
CPRS	3 (2-4)

Continuous variables are presented as mean ± standard deviation if normally distributed and median (interquartile range) if not normally distributed. Categorical variables are presented as number of patients (%). OCT, optical coherence tomography; CPRS, coronary plaque risk score.

CCs, macrophage infiltration, microchannels, calcification angle >90°, and microcalcifications. Each high-risk feature carries 1 point. Therefore, the possible range of the CPRS was 0-10 and is a sum of the number of high-risk plaque characteristics.

Blood tests and PCI

On admission, venous blood samples were collected to estimate routine laboratory parameters and inflammatory biomarkers including IL-6, TNF-α, hs-CRP, pentraxin 3, VEGF, and MCP-1. PCI was performed using standard procedures. Pre-dilatation was performed using a balloon, and post-dilatation was performed at the discretion of each operator.

Clinical outcomes

The primary clinical outcome was the rate of TLR within 15 months of follow-up. TLR was defined as any repeated PCI or coronary artery bypass grafting of the target lesion related to either: 1) ischemic symptoms and/or myocardial ischemia demonstrated by functional test and ≥50% diameter stenosis by quantitative angiographic assessment; or 2) any revascularization of a ≥70% diameter stenosis by quantitative angiographic assessment [13, 14].

Statistical analyses

Normally distributed data are expressed as mean ± standard deviation, and non-normally distributed data are expressed as median and interquartile range. Patients were divided into the low CPRS or high CPRS groups based on their CPRS. Comparisons of differences between the two groups were performed using Student *t*-tests or Mann-Whitney U tests for continuous variables and Pearson chi-square tests or Fisher's exact tests for categorical variables. A multivariable linear regression analysis was performed for variables with P<0.10 in the univariable linear regression analysis to explore the strongest determinants of CPRS. The relationship between the variables and TLR was evaluated using univariable logistic regression analysis. All tests were two-tailed, and a *P*-value <0.05 was considered statistically significant. All analyses were performed using Stata IC version 16 (StataCorp, College Station, TX, USA).

Results

Baseline characteristics

Morphological features of coronary plaques detected using OCT revealed that the median CPRS was 3 (2-4) (**Table 1**). Patients were divided into the low CPRS (CPRS ≤3) and high CPRS (CPRS ≥4) groups based on the median value of CPRS. The clinical characteristics of the patients are summarized in **Table 2**. Patients with a high CPRS were more likely to be female and have a higher serum IL-6 level than those with a low CPRS. There were no significant differences in age, comorbid chronic kidney disease, cholesterol profile, and hemoglobin A1c levels between the groups.

Relationship between coronary plaque morphology and inflammatory biomarkers

Multivariable linear regression analyses demonstrated that serum MCP-1 level was independently associated with CPRS (P=0.020) (**Table 3**). Associations between some biomarkers and morphological features of plaques were also observed. IL-6 level was associated with calcified nodule, calcification, and microcalcifications (P=0.049, P=0.033, and P=0.017, res-

Table 2. Baseline characteristics according to the CPRS

Variable	Overall (n=30)	Low CPRS (n=22)	High CPRS (n=8)	*P*-value
Age, years	69.8±8.8	69.8±8.7	69.8±9.8	1.0
Male, n (%)	20 (67)	17 (77)	3 (38)	0.041
Diabetes mellitus, n (%)	14 (47)	9 (41)	5 (63)	0.42
Hypertension, n (%)	29 (97)	21 (95)	8 (100)	1.0
Dyslipidemia, n (%)	28 (93)	21 (95)	7 (88)	0.47
Chronic kidney disease, n (%)	16 (53)	11 (50)	5 (63)	0.69
Current smoker, n (%)	5 (17)	3 (14)	2 (25)	0.59
Family history of coronary artery disease, n (%)	5 (17)	4 (18)	1 (13)	1.0
History of PCI or CABG, n (%)	18 (60)	14 (64)	4 (50)	0.68
History of CI or carotid artery stenosis, n (%)	12 (40)	10 (45)	2 (25)	0.42
Oral medication on admission, n (%)				
Prior aspirin use	30 (100)	22 (100)	8 (100)	-
Prior clopidogrel use	25 (83)	18 (82)	7 (88)	1.0
Prior prasugrel use	4 (13)	3 (14)	1 (13)	1.0
Prior beta blocker use	16 (53)	11 (50)	5 (63)	0.69
Prior ACEI or ARB	19 (63)	14 (64)	5 (63)	1.0
Prior statin use	26 (87)	20 (91)	6 (75)	0.28
Laboratory tests				
Hemoglobin, g/dL	12.8±1.6	13.1±1.5	11.9±1.6	0.072
White blood cell count, /μL	6,100 (5,000-7,000)	6,100 (5,300-7,000)	5,300 (4,150-6,750)	0.35
CRP, mg/dL	0.12 (0.04-0.17)	0.09 (0.04-0.15)	0.12 (0.07-1.06)	0.37
Total protein, g/dL	7.1 (6.7-7.4)	7.0 (6.7-7.4)	7.1 (6.7-7.4)	0.94
Albumin, g/dL	4.2 (4.0-4.4)	4.2 (4.0-4.4)	4.2 (3.6-4.4)	0.56
Creatinine, mg/dL	0.95 (0.84-1.11)	0.97 (0.84-1.07)	0.86 (0.78-4.70)	0.87
eGFR, mL/min	50.8±22.3	54.7±19.6	40.1±27.2	0.114
Calcium, mg/dL	9.3±0.4	9.2±0.4	9.5±0.4	0.144
LDL-C, mg/dL	80 (63-96)	80 (62-96)	80 (71-100)	0.45
Triglyceride, mg/dL	111 (78-171)	113 (78-175)	92 (77-124)	0.40
Glucose, mg/dL	118 (108-132)	120 (107-132)	114 (110-127)	0.71
HbA1c, %	6.2 (5.8-6.9)	6.1 (5.8-6.8)	6.8 (5.6-7.3)	0.45
IL-6, pg/mL	3.0 (1.6-5.1)	2.4 (1.3-3.6)	4.6 (3.0-13.7)	0.033
TNF-α, pg/mL	1.24 (0.90-1.56)	1.14 (0.79-1.51)	1.37 (0.97-2.07)	0.34
hs-CRP, ng/mL	668 (375-1460)	550 (279-1,390)	920 (616-6,500)	0.140
Pentraxin 3, ng/mL	1.96 (1.37-2.62)	1.80 (1.31-2.25)	2.63 (1.76-3.66)	0.116
VEGF >20 pg/mL, n (%)	7 (23)	6 (27)	1 (13)	0.40
MCP-1, pg/mL	188 (155-230)	187 (153-211)	234 (178-289)	0.075
Target lesion, n (%)				0.46
Left anterior descending artery	19 (63)	14 (64)	5 (63)	
Left circumflex artery	3 (10)	3 (14)	0	
Right coronary artery	8 (27)	5 (23)	3 (38)	
Balloon angioplasty, n (%)	30 (100)	22 (100)	8 (100)	-
Stent implantation, n (%)	17 (57)	14 (64)	3 (38)	0.20
Drug-coated balloon, n (%)	13 (43)	8 (36)	5 (63)	0.20

Continuous variables are presented as mean ± standard deviation if normally distributed and as median (interquartile range) if not normally distributed. Categorical variables are presented as the number of patients (%). CPRS, coronary plaque risk score; PCI, percutaneous coronary intervention; CABG, coronary artery bypass grafting; CI, cerebral infarction; ACEI, angiotensin converting enzyme inhibitor; ARB, angiotensin II receptor blocker; CRP, C-reactive protein; eGFR, estimated glomerular filtration rate; LDL-C, low-density lipoprotein cholesterol; HbA1c, hemoglobin A1c; IL-6, Interleukin-6; TNF-α, tumor necrosis factor-alpha; hs-CRP, high-sensitivity C-reactive protein; VEGF, vascular endothelial growth factor; MCP-1, monocyte chemoattractant protein-1.

pectively, **Table 4**); hs-CRP level was associated with lipid-rich plaque (P=0.014, **Table 4**); pentraxin 3 level was associated with microcalcifications (P=0.025, **Table 4**); and MCP-1 level

Table 3. Linear regression analyses of the coronary plaque risk score

Variables	Univariable		Multivariable	
	β coefficient	*P*-value	β coefficient	*P*-value
Hemoglobin	-1.77	0.29	Not selected	-
Log WBC	-0.09	0.55	Not selected	-
CRP	0.42	0.165	Not selected	-
Log eGFR	-0.67	0.040	-1.14	0.74
IL-6	0.08	0.058	0.01	0.86
TNF-α	0.48	0.25	Not selected	-
Log hs-CRP	0.31	0.109	Not selected	-
Pentraxin 3	0.25	0.188	Not selected	-
Log MCP-1	2.31	0.001	2.04	0.020

WBC, white blood cell count; CRP, C-reactive protein; eGFR, estimated glomerular filtration rate; IL-6, Interleukin-6; TNF-α, tumor necrosis factor-alpha; hs-CRP, high-sensitivity C-reactive protein; MCP-1, monocyte chemoattractant protein-1.

was associated with calcified nodule, lipid-rich plaque, and microcalcifications (P=0.035, P=0.033, and P=0.019, respectively, **Table 4**). No other association between inflammatory biomarkers and plaque rupture, macrophage infiltration, CCs, and microchannels was observed. Univariate linear regression analyses revealed that serum levels of CRP, IL-6, TNF-α, and hs-CRP were correlated with MCP-1 levels (P=0.039, P=0.001, P=0.001, and P=0.024, respectively, **Table 5**).

CPRS and the primary outcome

At the 15-month follow-up, TLR was noted in 6 (20%) patients. The incidence of TLR at 15 months was significantly higher in the high CPRS group than in the low CPRS group (50.0% vs. 9.1%, P=0.029, **Figure 3**). In univariate logistic regression analyses, CPRS was associated with TLR (odds ratio, 10.0; 95% confidence interval, 1.34-74.5, P=0.025, **Table 6**); however, the inflammatory biomarkers did not achieve a statistically significant association.

Discussion

In the current study, we found that a high CPRS was associated with a high incidence of TLR, and several inflammatory biomarkers, including MCP-1, were related to the morphological features of high-risk coronary plaques. Our findings highlight the significance of comprehensive assessments of the morphology of high-risk coronary plaques using OCT for further risk stratification in patients with CCS.

Several factors might explain the higher CPRS in patients with TLR than in those without TLR. First, among the 10 coronary plaque characteristics used for CPRS quantification, plaque rupture, plaque erosion, calcified nodule, lipid-rich plaque, macrophage infiltration, TCFA, CCs, microchannels, and microcalcifications were associated with coronary plaque instability. Lesions with plaque rupture, plaque erosion, or a calcified nodule have been reported to be common causes of acute coronary syndrome [15]. Previous studies have indicated that fibroatheroma with a large lipid-rich plaque represents one of the high-risk characteristics for adverse coronary events [16]. Several types of matrix metalloproteinases produced by macrophages digest the collagen of fibrous tissue, thus causing the plaque's mechanical instability [17]. Microchannel proliferation in atheromatous coronary plaques plays a pivotal role in atherosclerotic progression by increasing the blood flow in the plaque and, consequently, causing the infiltration of inflammatory cells including foam cells and cytokines [18]. When CCs are generated in a fibrous cap of the intima, the circumferential stress of the intimal plaque could substantially rise and increase the risk of fibrous cap disruption [19]. When microcalcifications are clustered along the tensile axis of the cap in the coronary arteries, they may increase the local structural stress by over five times, thus leading to plaque instability [20]. Second, a calcification angle >90°, which is considered a high degree of calcification, and a calcified nodule may cause inadequate lesion preparation and subsequent incomplete asymmetrical stent expansion, thus leading to restenosis after PCI [21]. The CPRS is a useful parameter that is related to both plaque instability and suboptimal stent expansion. A recent study showed the non-inferiority of a robotic-assisted PCI system versus a traditional PCI regarding radiation exposure to the assistant, fluoroscopy time, procedural time, and contrast volume in selected patients [22]. Artificial intelligence systems

Table 4. Association of inflammatory biomarkers with calcified nodules, lipid-rich plaque, calcification, and microcalcification

Inflammatory marker	Calcified nodule		*P*-value	Lipid-rich plaque		*P*-value	Calcification		*P*-value	Microcalcification		*P*-value
	Absent (n=27)	Present (n=3)		Absent (n=13)	Present (n=17)		Absent (n=17)	Present (n=13)		Absent (n=21)	Present (n=9)	
IL-6, pg/mL	2.5 (1.4-4.1)	5.3 (3.8-28.4)	0.049	3.1 (1.6-4.1)	2.5 (1.8-5.3)	0.92	2.2 (1.3-3.1)	3.8 (3.0-7.2)	0.033	2.4 (1.6-3.1)	5.3 (3.8-8.5)	0.017
TNF-α, pg/mL	1.22 (0.79-1.51)	1.56 (1.01-2.58)	0.20	0.97 (0.75-1.33)	1.43 (0.99-1.58)	0.14	1.05 (0.90-1.50)	1.32 (0.93-1.83)	0.25	0.99 (0.79-1.50)	1.48 (1.26-2.44)	0.054
hs-CRP, ng/mL	638 (279-1,460)	697 (534-30,800)	0.39	456 (235-638)	1220 (534-3810)	0.014	710 (456-1390)	534 (279-2300)	0.98	603 (375-1220)	1130 (534-4600)	0.21
Pentraxin 3, ng/mL	1.85 (1.31-2.31)	2.63 (2.62-3.39)	0.078	1.85 (1.30-2.04)	2.17 (1.66-3.39)	0.107	1.96 (1.47-2.17)	2.31 (1.31-3.39)	0.60	1.74 (1.31-2.10)	2.63 (2.31-3.76)	0.025
VEGF >20 pg/mL, n (%)	7 (26)	0	1.0	1 (8)	6 (35)	0.104	4 (24)	3 (23)	1.0	4 (19)	3 (33)	0.64
MCP-1, pg/mL	186 (153-214)	287 (223-291)	0.035	178 (145-187)	214 (174-275)	0.033	174 (125-214)	195 (181-245)	0.079	178 (145-198)	223 (195-287)	0.019

Continuous variables are presented as median (interquartile range). Categorical variables are presented as number of patients (%). IL-6, interleukin-6; TNF-α, tumor necrosis factor alpha; hs-CRP, high-sensitivity C-reactive protein; VEGF, vascular endothelial growth factor; MCP-1, monocyte chemoattractant protein-1.

Table 5. Linear regression analyses for factors associated with log MCP-1

Variables	Univariable	
	β coefficient	*P*-value
Log WBC	0.01	0.86
CRP	0.15	0.039
IL-6	7.45	0.001
TNF-α	0.31	0.001
Log hs-CRP	0.10	0.024
Pentraxin-3	0.06	0.21

IL-6, interleukin-6; CRP, C-reactive protein; TNF-α, tumor necrosis factor alpha; hs-CRP, high-sensitivity C-reactive protein; WBC, white blood cells.

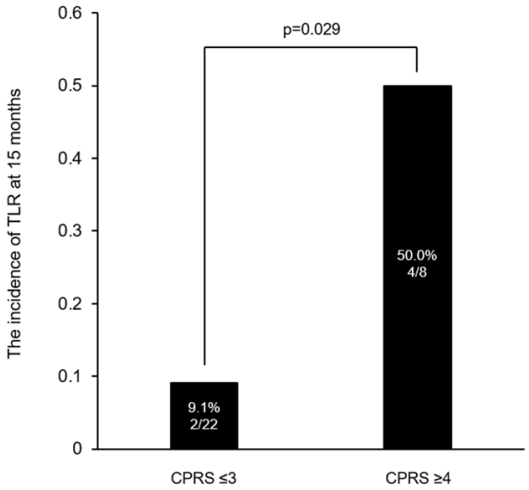

Figure 3. Comparison of TLR at 15 months between patients with CPRS ≤3 and patients with CPRS ≥4. TLR, target lesion revascularization; CPRS, coronary plaque risk score.

using CPRS by OCT may also be useful for increasing the effect of a prediction model of TLR.

Inflammation plays an important role in the formation of atherosclerotic plaques. Several inflammatory biomarkers have been extensively studied and have been found to predict CAD development. Remarkably, hs-CRP is one of the most important inflammatory biomarkers that indicate an increased risk of CAD [23]. However, there is no direct relationship between hs-CRP levels and CPRS or TLR (**Tables 3** and **6**). Interestingly, MCP-1 level was significantly associated with CRPS in the present study. As shown in **Table 5**, IL-6 level was correlated with MCP-1 level, which is in accordance with a previous study showing that IL-6 level increases plaque instability by activating macrophages to secrete MCP-1 [24]. Furthermore, TNF receptor-1 activity increases MCP-1 expression in both pre-atherosclerotic and advanced atheromatous lesions [25]. Therefore, MCP-1 might be useful in detecting high-risk coronary plaques that are associated with future coronary events in patients with CCS, even when OCT is not available for PCI.

Limitations

This study has some limitations. First, the current prospective, observational study performed at a single university hospital included a small sample size, thereby limiting the generalizability of the findings and the statistical power for detecting differences. Therefore, large-scale multicenter prospective studies are warranted to confirm the associations of CPRS with inflammatory biomarkers and clinical outcomes. Second, there is an inherent discrepancy between plaque characteristics evaluated using OCT and histopathological findings [26]. For example, in this study, we were unable to perform adequate assessments of calcification because the near-infrared signal from the OCT transducer cannot pass through a lipid-rich plaque and cannot help visualize calcification outside the lipid-rich plaque. Third, patients with chronic total occlusion (CTO), who potentially have more severe atherosclerotic lesions, were not included in the current study because PCI for CTO using OCT may be technically difficult.

Conclusions

High CPRS was associated with TLR at 15 months after PCI in patients with CCS and a high MCP-1 level. Our findings suggest the potential value of evaluating CPRS for further risk stratification in the aforementioned type of patients.

Acknowledgements

The authors are grateful for the contributions of all investigators, laboratory technicians, and clinical research coordinators involved in this study. This study was supported by a Grant-in-Aid for Research Activity Start-up (Japan Society for the Promotion of Science KAKENHI, 19K23931 T.K.) and the research grant from

Table 6. Logistic regression analyses for target lesion revascularization at 15 months

Variable	Target lesion revascularization at 15 months			
	Absent (n=24)	Present (n=6)	OR (crude) (95% CI)	*P*-value
Age, years	69.2±9.2	72.0±7.5	1.04 (0.93-1.16)	0.49
Male, n (%)	17 (71)	3 (50)	0.41 (0.07-2.56)	0.34
Diabetes mellitus, n (%)	10 (42)	4 (67)	2.80 (0.43-18.4)	0.28
Hypertension, n (%)	23 (96)	6 (100)	-	-
Dyslipidemia, n (%)	23 (96)	5 (83)	0.22 (0.01-4.09)	0.31
Chronic kidney disease, n (%)	12 (50)	4 (67)	2.00 (0.31-13.1)	0.47
Current smoker, n (%)	3 (13)	2 (33)	3.50 (0.44-28.1)	0.24
Family history of coronary artery disease, n (%)	5 (21)	0	-	-
History of PCI or CABG, n (%)	14 (58)	4 (67)	1.43 (0.22-9.38)	0.71
History of cerebral infarction or carotid artery stenosis, n (%)	9 (38)	3 (50)	1.67 (0.28-10.1)	0.58
Oral medication on admission, n (%)				
Prior aspirin use	24 (100)	6 (100)	-	-
Prior clopidogrel use	21 (88)	4 (66)	0.29 (0.04-2.30)	0.24
Prior prasugrel use	2 (8)	2 (33)	5.50 (0.59-51.2)	0.134
Prior beta blocker use	14 (58)	2 (33)	0.36 (0.05-2.34)	0.28
Prior ACEI or ARB	16 (67)	3 (50)	0.50 (0.08-3.06)	0.45
Prior statin use	21 (88)	5 (83)	0.71 (0.06-8.40)	0.79
Laboratory tests				
Hemoglobin, g/dL	12.9±1.5	12.1±1.7	0.70 (0.39-1.25)	0.23
White blood cell count, /μL	6,100 (5,150-7,250)	5,600 (4,200-6,300)	1.00 (1.00-1.00)	0.58
CRP, mg/dL	0.10 (0.04-0.16)	0.14 (0.03-0.29)	1.11 (0.43-2.87)	0.83
Total protein, g/dL	7.1 (6.7-7.4)	7.0 (6.8-7.1)	0.34 (0.05-2.26)	0.26
Albumin, g/dL	4.2 (4.0-4.4)	4.3 (4.1-4.4)	0.63 (0.12-3.45)	0.60
Creatinine, mg/dL	0.95 (0.83-1.09)	0.93 (0.85-4.38)	1.10 (0.74-1.63)	0.65
eGFR, mL/min	53.0±21.4	42.2±25.9	0.98 (0.94-1.02)	0.29
Uric acid, mg/dL	5.2±1.3	4.5±1.6	0.67 (0.32-1.40)	0.28
Calcium, mg/dL	9.3±0.5	9.4±0.4	2.45 (0.34-17.9)	0.38
LDL-C, mg/dL	78 (62-94)	87 (75-110)	1.02 (0.98-1.06)	0.28
Triglyceride, mg/dL	113 (78-173)	91 (76-118)	0.99 (0.97-1.00)	0.36
Glucose, mg/dL	119 (109-132)	113 (108-142)	1.02 (0.99-1.04)	0.26
HbA1c, %	6.1 (5.8-6.8)	6.7 (5.5-7.2)	1.88 (0.64-5.57)	0.25
IL-6, pg/mL	3.0 (1.9-4.6)	2.6 (1.3-5.3)	1.03 (0.90-1.18)	0.69
TNF-α, pg/mL	1.14 (0.85-1.55)	1.38 (1.01-1.56)	1.75 (0.46-6.74)	0.41
hs-CRP, ng/mL	623 (327-1340)	1044 (534-2300)	1.00 (1.00-1.00)	0.92
Pentraxin 3, ng/mL	1.91 (1.31-2.41)	2.47 (1.67-2.63)	1.12 (0.61-2.05)	0.37
VEGF >20 pg/mL, n (%)	5 (21)	2 (33)	1.90 (0.27-13.5)	0.52
MCP-1, pg/mL	182 (149-206)	227 (211-287)	1.02 (1.00-1.03)	0.061
Target lesion, n (%)				
Left anterior descending artery	14 (58)	5 (83)	3.57 (0.36-35.5)	0.28
Left circumflex artery	3 (13)	0	-	-
Right coronary artery	7 (29)	1 (17)	0.49 (0.05-4.94)	0.54
Balloon angioplasty, n (%)	24 (100)	6 (100)	-	-
Stent implantation, n (%)	14 (58)	3 (50)	0.71 (0.12-4.30)	0.71
Drug-coated balloon, n (%)	10 (42)	3 (50)	1.40 (0.23-8.42)	0.71
Coronary plaque risk score ≥4	4 (17)	4 (67)	10.0 (1.34-74.5)	0.025

Continuous variables are presented as mean ± standard deviation if normally distributed and median (interquartile range) if not normally distributed. Categorical variables are presented as number of patients (%). CI, confidence interval; OR, odds ratio. PCI, percutaneous coronary intervention; CABG, coronary artery bypass grafting; CI, cerebral infarction; ACEI, angiotensin converting enzyme inhibitor; ARB, angiotensin II receptor blocker; CRP, C-reactive protein; eGFR, estimated glomerular filtration rate; LDL-C, low-density lipoprotein cholesterol; HbA1c, hemoglobin A1c; IL-6, Interleukin-6; TNF-α, tumor necrosis factor-alpha; hs-CRP, high-sensitivity C-reactive protein; VEGF, vascular endothelial growth factor; MCP-1, monocyte chemoattractant protein-1.

The Ito foundation (The 27th Ito Foundation, T.K.).

The patients provided informed consent to participate in this study.

Disclosure of conflict of interest

None.

Abbreviations

OCT, optical coherence tomography; CCS, chronic coronary syndrome; PCI, percutaneous coronary intervention; CPRS, coronary plaque risk score; TLR, target lesion revascularization; MCP-1, monocyte chemoattractant protein-1; CAD, coronary artery disease; TCFA, thin-cap fibroatheroma; CCs, cholesterol crystals; DM, diabetes mellitus; IL, interleukin; TNF-α, tumor necrosis factor-alpha; hs-CRP, high-sensitivity C-reactive protein.

Address correspondence to: Dr. Takao Konishi, Department of Cardiovascular Medicine, Faculty of Medicine and Graduate School of Medicine, Hokkaido University, Kita 15, Nishi 7, Kita-ku, Sapporo, Hokkaido 060-8638, Japan. Tel: +81-11-706-6973; Fax: +81-11-706-7874; E-mail: takaokonishi0915@gmail.com

References

[1] Kastrati A and Cassese S. In-stent restenosis in the United States: time to enrich its treatment armamentarium. J Am Coll Cardiol 2020; 76: 1532-1535.

[2] Shlofmitz E, Iantorno M and Waksman R. Restenosis of drug-eluting stents: a new classification system based on disease mechanism to guide treatment and state-of-the-art review. Circ Cardiovasc Interv 2019; 12: e007023.

[3] Fabris E, Berta B, Roleder T, Hermanides RS, IJsselmuiden AJJ, Kauer F, Alfonso F, von Birgelen C, Escaned J, Camaro C, Kennedy MW, Pereira B, Magro M, Nef H, Reith S, Roleder-Dylewska M, Gasior P, Malinowski K, De Luca G, Garcia-Garcia HM, Granada JF, Wojakowski W and Kedhi E. Thin-cap fibroatheroma rather than any lipid plaques increases the risk of cardiovascular events in diabetic patients: insights from the COMBINE OCT-FFR trial. Circ Cardiovasc Interv 2022; 15: e011728.

[4] Kedhi E, Berta B, Roleder T, Hermanides RS, Fabris E, IJsselmuiden AJJ, Kauer F, Alfonso F, von Birgelen C, Escaned J, Camaro C, Kennedy MW, Pereira B, Magro M, Nef H, Reith S, Al Nooryani A, Rivero F, Malinowski K, De Luca G, Garcia Garcia H, Granada JF and Wojakowski W. Thin-cap fibroatheroma predicts clinical events in diabetic patients with normal fractional flow reserve: the COMBINE OCT-FFR trial. Eur Heart J 2021; 42: 4671-4679.

[5] Xing L, Higuma T, Wang Z, Aguirre AD, Mizuno K, Takano M, Dauerman HL, Park SJ, Jang Y, Kim CJ, Kim SJ, Choi SY, Itoh T, Uemura S, Lowe H, Walters DL, Barlis P, Lee S, Lerman A, Toma C, Tan JWC, Yamamoto E, Bryniarski K, Dai J, Zanchin T, Zhang S, Yu B, Lee H, Fujimoto J, Fuster V and Jang IK. Clinical significance of lipid-rich plaque detected by optical coherence tomography: a 4-year follow-up study. J Am Coll Cardiol 2017; 69: 2502-2513.

[6] Kogo T, Hiro T, Kitano D, Takayama T, Fukamachi D, Morikawa T, Sudo M and Okumura Y. Macrophage accumulation within coronary arterial wall in diabetic patients with acute coronary syndrome: a study with in-vivo intravascular imaging modalities. Cardiovasc Diabetol 2020; 19: 135.

[7] Antonopoulos AS, Angelopoulos A, Papanikolaou P, Simantiris S, Oikonomou EK, Vamvakaris K, Koumpoura A, Farmaki M, Trivella M, Vlachopoulos C, Tsioufis K, Antoniades C and Tousoulis D. Biomarkers of vascular inflammation for cardiovascular risk prognostication: a meta-analysis. JACC Cardiovasc Imaging 2022; 15: 460-471.

[8] Au Yeung SL, Lam HSHS and Schooling CM. Vascular endothelial growth factor and ischemic heart disease risk: a mendelian randomization study. J Am Heart Assoc 2017; 6: e005619.

[9] Georgakis MK, de Lemos JA, Ayers C, Wang B, Björkbacka H, Pana TA, Thorand B, Sun C, Fani L, Malik R, Dupuis J, Engström G, Orho-Melander M, Melander O, Boekholdt SM, Zierer A, Elhadad MA, Koenig W, Herder C, Hoogeveen RC, Kavousi M, Ballantyne CM, Peters A, Myint PK, Nilsson J, Benjamin EJ and Dichgans M. Association of circulating monocyte chemoattractant protein-1 levels with cardiovascular mortality: a meta-analysis of population-based studies. JAMA Cardiol 2021; 6: 587-592.

[10] Tearney GJ, Regar E, Akasaka T, Adriaenssens T, Barlis P, Bezerra HG, Bouma B, Bruining N, Cho JM, Chowdhary S, Costa MA, de Silva R, Dijkstra J, Di Mario C, Dudek D, Falk E, Feldman MD, Fitzgerald P, Garcia-Garcia HM, Gonzalo N, Granada JF, Guagliumi G, Holm NR, Honda Y, Ikeno F, Kawasaki M, Kochman J, Koltowski L, Kubo T, Kume T, Kyono H, Lam CC, Lamouche G, Lee DP, Leon MB, Maehara A, Manfrini O, Mintz GS, Mizuno K, Morel MA, Nadkarni S, Okura H, Otake H, Pietrasik A, Prati F, Raber L, Radu MD, Rieber J, Riga M, Rollins A, Rosenberg M, Sirbu V, Serruys PW, Shimada K, Shinke T, Shite J, Siegel E, Sonoda S, Suter M, Takarada S, Tanaka A, Terashima M, Thim T, Uemura S, Ughi GJ, van Beusekom HM, van der Steen AF, van Es GA, van Soest G, Virmani R, Waxman S, Weissman NJ and Weisz G;

International Working Group for Intravascular Optical Coherence Tomography (IWG-IVOCT). Consensus standards for acquisition, measurement, and reporting of intravascular optical coherence tomography studies: a report from the International Working Group for Intravascular Optical Coherence Tomography Standardization and Validation. J Am Coll Cardiol 2012; 59: 1058-1072.

[11] Higuma T, Soeda T, Abe N, Yamada M, Yokoyama H, Shibutani S, Vergallo R, Minami Y, Ong DS, Lee H, Okumura K and Jang IK. A combined optical coherence tomography and intravascular ultrasound study on plaque rupture, plaque erosion, and calcified nodule in patients with ST-segment elevation myocardial infarction: incidence, morphologic characteristics, and outcomes after percutaneous coronary intervention. JACC Cardiovasc Interv 2015; 8: 1166-1176.

[12] Milzi A, Burgmaier M, Burgmaier K, Hellmich M, Marx N and Reith S. Type 2 diabetes mellitus is associated with a lower fibrous cap thickness but has no impact on calcification morphology: an intracoronary optical coherence tomography study. Cardiovasc Diabetol 2017; 16: 152.

[13] Garcia-Garcia HM, McFadden EP, Farb A, Mehran R, Stone GW, Spertus J, Onuma Y, Morel MA, van Es GA, Zuckerman B, Fearon WF, Taggart D, Kappetein AP, Krucoff MW, Vranckx P, Windecker S, Cutlip D and Serruys PW; Academic Research Consortium. Standardized end point definitions for coronary intervention trials: the academic research consortium-2 consensus document. Eur Heart J 2018; 39: 2192-2207.

[14] Kandzari DE, Koolen JJ, Doros G, Garcia-Garcia HM, Bennett J, Roguin A, Gharib EG, Cutlip DE and Waksman R; BIOFLOW V Investigators. Ultrathin bioresorbable-polymer sirolimus-eluting stents versus thin durable-polymer everolimus-eluting stents for coronary revascularization: 3-year outcomes from the randomized BIOFLOW V trial. JACC Cardiovasc Interv 2020; 13: 1343-1353.

[15] Virmani R, Burke AP, Farb A and Kolodgie FD. Pathology of the vulnerable plaque. J Am Coll Cardiol 2006; 47 Suppl: C13-18.

[16] Virmani R, Kolodgie FD, Burke AP, Farb A and Schwartz SM. Lessons from sudden coronary death: a comprehensive morphological classification scheme for atherosclerotic lesions. Arterioscler Thromb Vasc Biol 2000; 20: 1262-1275.

[17] Newby AC, George SJ, Ismail Y, Johnson JL, Sala-Newby GB and Thomas AC. Vulnerable atherosclerotic plaque metalloproteinases and foam cell phenotypes. Thromb Haemost 2009; 101: 1006-1011.

[18] Badimon L, Padró T and Vilahur G. Atherosclerosis, platelets and thrombosis in acute ischaemic heart disease. Eur Heart J Acute Cardiovasc Care 2012; 1: 60-74.

[19] Katayama Y, Tanaka A, Taruya A, Kashiwagi M, Nishiguchi T, Ozaki Y, Matsuo Y, Kitabata H, Kubo T, Shimada E, Kondo T and Akasaka T. Feasibility and clinical significance of in vivo cholesterol crystal detection using optical coherence tomography. Arterioscler Thromb Vasc Biol 2020; 40: 220-229.

[20] Kelly-Arnold A, Maldonado N, Laudier D, Aikawa E, Cardoso L and Weinbaum S. Revised microcalcification hypothesis for fibrous cap rupture in human coronary arteries. Proc Natl Acad Sci U S A 2013; 110: 10741-10746.

[21] Krajcer Z and Costello B. Clinical impact of calcified nodules in patients with heavily calcified lesions requiring rotational atherectomy. Catheter Cardiovasc Interv 2021; 97: 20-21.

[22] Kagiyama K, Mitsutake Y, Ueno T, Sakai S, Nakamura T, Yamaji K, Ishimatsu T, Sasaki M, Chibana H, Itaya N, Sasaki KI and Fukumoto Y. Successful introduction of robotic-assisted percutaneous coronary intervention system into Japanese clinical practice: a first-year survey at single center. Heart Vessels 2021; 36: 955-964.

[23] Pai JK, Pischon T, Ma J, Manson JE, Hankinson SE, Joshipura K, Curhan GC, Rifai N, Cannuscio CC, Stampfer MJ and Rimm EB. Inflammatory markers and the risk of coronary heart disease in men and women. N Engl J Med 2004; 351: 2599-2610.

[24] Biswas P, Delfanti F, Bernasconi S, Mengozzi M, Cota M, Polentarutti N, Mantovani A, Lazzarin A, Sozzani S and Poli G. Interleukin-6 induces monocyte chemotactic protein-1 in peripheral blood mononuclear cells and in the U937 cell line. Blood 1998; 91: 258-265.

[25] Zhang L, Peppel K, Sivashanmugam P, Orman ES, Brian L, Exum ST and Freedman NJ. Expression of tumor necrosis factor receptor-1 in arterial wall cells promotes atherosclerosis. Arterioscler Thromb Vasc Biol 2007; 27: 1087-1094.

[26] Phipps JE, Hoyt T, Vela D, Wang T, Michalek JE, Buja LM, Jang IK, Milner TE and Feldman MD. Diagnosis of thin-capped fibroatheromas in tntravascular optical coherence tomography images: effects of light scattering. Circ Cardiovasc Interv 2016; 9: 10.1161/CIRCINTERVENTIONS.115.003163 e003163.